A Letters Journal Exploring the Frontiers of Physics

July 2007

EPL, **79** (2007) 16001 www.epljournal.org
doi: 10.1209/0295-5075/79/16001

# Mesoscopic mismatch as a driving force for modified morphology above percolation

R. Dana and Y. Manassen

*Department of Physics, Ben-Gurion University of the Negev - P.O. Box 653, Beer Sheva, 84105, Israel*

received 15 November 2006; accepted in final form 21 May 2007
published online 11 June 2007

PACS 68.35.Gy – Mechanical properties; surface strains
PACS 68.37.Ef – Scanning tunneling microscopy (including chemistry induced with STM)
PACS 68.65.-k – Low-dimensional, mesoscopic, and nanoscale systems: structure and nonelectronic properties

**Abstract** – The steady-state morphology of submonolayer Si/Si(111)$7 \times 7$ islands is characterized by a size-dependent transition from compact through ramified to 1D-like forms. The transition is described by the linear-chain model (LCM), which explains this shape transition in strained heteroepitaxial layers, as a mechanism for strain relaxation without dislocations. We found that above the percolation coverage $\theta_c$, the entire structure adopts new steady-state morphology and reduces its typical width by a factor of $e$, to its optimal-energy value. The LCM predicts this value as the asymptotic behavior for infinite elongated islands. Our experimental results, which are supported by energy calculations, confirm the LCM predictions for the first time in homoepitaxy. These results are explained by a size-dependent mesoscopic mismatch between the islands and the substrate.



Percolation is a mathematical model, describing a geometrical phase transition, in infinite disordered systems. By randomly filling sites on an infinite 2D lattice, the site percolation threshold $p_c$ is defined as the site occupation probability where for the first time an infinite island spans the entire system. Percolation was extensively investigated, both theoretically and experimentally (see [1] for introduction) and was implemented in many fields of research. It is defined for many characteristics like; different connectivity rules and lattice symmetries, from 1 to $n$ dimensions, for discrete or continuous systems and for random or correlated occupation probabilities. In percolation, a correlation or pair-connectivity function is defined as the probability that a site a distance $r$ apart from an occupied site belongs to the same cluster. A geometrical typical length, called the correlation or connectivity length $\xi$ is than defined, for 2D, as some average distance of two sites belonging to the same island. Thus, as the critical occupation probability $p_c$ is being approached, $\xi$ is expected to experience geometrical phase transition and to diverge. $\xi$ itself and statistical quantities defined by it are also subject to scaling laws when $p \to p_c$, but, the morphology of the percolating islands has not been predicted or observed previously to be affected by this phase transition. In this letter, we present experimental results showing a strain-driven morphological transition associated with the geometrical critical point of percolation. The transition is characterized by a reduction of the typical island width $w$ by a factor of $e$ above the percolation threshold. The characterization of percolative and ramified geometries in surface overlayer systems is a well-established field of research (see [2] for report). Specifically, in this work, the appearance of the factor $e$, led us to the linear chain model (LCM) first introduced by Tersoff and Tromp (TT) [3]. The LCM describes island formation in strained heteroepitaxial layers, as a mechanism for strain relaxation without dislocations. TT described the strained islands by applying elastic monopoles at the border of the deposit. By minimizing the total energy with respect to the island geometry, they found an optimal island size $\alpha_0^2$ at the optimal tradeoff between extra surface and interface energy and the energy gained due to elastic relaxation. They also showed that compact islands are stable as long as their linear size $\leqslant e\alpha_0$. However, once an island grows beyond its optimal area $\alpha_0^2$ by a factor of $e^2$, a morphological transition to rectangular shape is observed. The LCM also predicts an asymptotic convergence to the optimal width $\alpha_0$ as the island length grows to infinity. This is a fundamental

feature that connects the LCM to percolation. On the one hand, percolation is defined as the coverage where an infinite island is formed. On the other hand, the LCM predicts the asymptotic island width value as the island length grows to infinity. Thus, when a percolating island system can be described by the LCM, the asymptotic value is expected to be found when the percolation threshold is being approached. Our data taken from both sides of the percolation threshold, (*i.e.*, before and after an infinite island is formed), are consistent with this prediction. We also demonstrate, for the first time known to us, the validity of this model for homoepitexial islands. By growing nanoscale Si/Si(111)$7\times7$ islands, we argue that a finite-size misfit, now long recognized (theoretically and experimentally) [4–8] as effective also in homoepitaxy, is responsible for the presence of strain forces. Strain forces are essential in justifying the existence of the shape transition predicted by the LCM.

In this letter, we will first present the experimental results showing the morphological modification of the typical island width. The analysis will start by calculating the site-occupation correlation function $g_\theta(r)$ (differ from the pair-connectivity function). The determination of $g_\theta(r)$ *vs.* $r$ will yield expected and unexpected results. The expected result is that above a typical length, the island system can be regarded as uncorrelated or random. The unexpected result is that the typical island width reduces dramatically after the percolation threshold is being crossed. We will continue by verifying that the large scale morphology can be modeled by percolation. The expected transition from compact to fractal behavior will be presented here along with estimation of two critical exponents, the fractal dimension $D$ and the cluster number exponent $\tau$. In the main part we will address the new steady-state morphology found above $\theta_c$. By using an adapted LCM version for 2D ramified islands, the transition from compact through ramified to linear-chain islands will be presented and the typical values of these transitions will be estimated. Following that, the reduction of the typical island width by a factor of $e$ will be introduced. We shall also discuss the connection to percolation via the formation of infinite island and the appearance of two characteristic lengths which are the correlation/connectivity length $\xi$ for the large scale morphology and the typical width $w$ for the small scale morphology. To further support our finding, we include an energy calculation relevant for Si homoepitaxy. Finally, since it is the first time that the LCM is being applied in homoepitaxy, we shall conclude by introducing the finite-size misfit in strain mesoscopic islands in our explanation.

In the experiment, silicon atoms were evaporated on top of a Si(111)$7\times7$ surface at room temperature. After solid phase epitaxy, the substrate was annealed to 550 °C and a system of 2D islands was formed. In less than 3 minutes the system reached a steady state and further heating, even to temperatures up to 700 °C, did not change the morphology. Images from different submonolayer coverages were collected by a custom made UHV-STM applying a sample bias of +2 V and at a constant current of approx 1 nA. The images were digitized to a binary contrast with 1 and 0 for occupied (white) and vacant (black) sites, respectively, and so, we could analyze the STM images in analogy to site percolation problem. Since the Si(111) surface can show domains of different reconstructions with formed islands, the results are presented using the Si(111) lattice units (LU), for the sake of uniformity. To demonstrate our findings, data of three different coverages ($\theta=0.446$, 0.534 and 0.566) at a total of 3459 islands were analyzed. The images (see fig. 1) show that percolation sets in between 0.534 and 0.566, and that a transition to a significant narrower island width occurs while crossing this threshold. We shall start the analysis by calculating $g_\theta(r)$ for the percolating island system.

The site percolation problem can be defined by the site occupation variable $\theta_i$ at the sites $\{i\}$. $\theta_i$ take on the values 1 and 0 corresponding to occupied or vacant sites, respectively. Thus, the site occupation probability is defined by the statistical average $\theta=\langle\theta_i\rangle$ on realizations of $\{\theta_i\}$. One way to characterize island morphology and estimate the typical width is to calculate the site occupation correlation function $g_\theta(r)$:

$$g_\theta(r)=\langle\theta,\theta_j\rangle-\langle\theta_i\rangle\langle\theta_j\rangle\,. \tag{1}$$

By considering an homogenous and isotropic system, $g_\theta(r)$ is a scalar function of the distance $r=|r_i-r_j|$ alone, where $\langle\theta,\theta_j\rangle$ measure the average probability that if site $i$ is occupied so is site $j$ (a distance $r$ apart), and $\langle\theta_i\rangle\langle\theta_j\rangle\equiv\theta^2$. In random percolation (RP), $g_\theta(r)=\theta(1-\theta)\delta_{ij}$, and so, $g_\theta(r)\equiv0$ unless $r=0$. When correlations do exist, $g_\theta(r)$ is a circularly average measurement of the correlation changes with the distance $r$.

Figure 2 shows $g_\theta(r)$ calculated from our data at $\theta=0.446$, $0.534<\theta_c$ and $\theta=0.566>\theta_c$. We see that beyond the first secondary maximum, which estimates the distance between to adjusting trench centers, $g_\theta(r)$ exhibit sinusoidal fluctuations near 0. Hence, as expected, it is already after one cycle of the oscillatory island-trench morphology that the system shows no correlations and can be regarded as random. For the first zero, which is one estimation of the typical island width $w$, we see an unexpected jump towards a smaller value when moving from $\theta<\theta_c$ to $\theta>\theta_c$. This finding means that on the nanoscale, the typical island width experiences a morphological transition when crossing the percolation threshold. We shall go on and verify that percolation can model the large scale morphology.

Since the morphology is driven by postdeposition dynamics, correlated percolation models, (for example annealed percolation [9]), can be applied in order to characterize the critical behavior of the system (proven to be in the same universality class of RP). Nevertheless, in this letter we do not focus on the percolation characteristics of our system, and since the formation of an

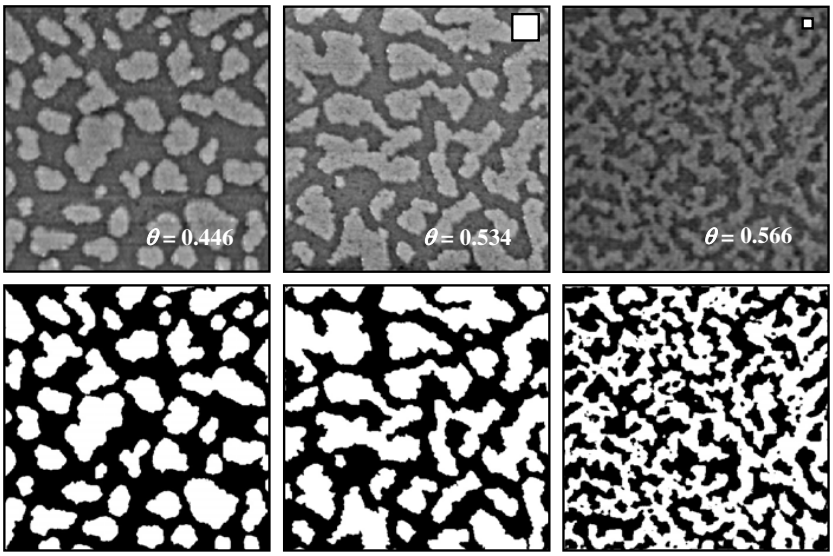


Fig. 1: STM images of silicon island on Si(111) $7\times7$ and their B& W matrix (white = occupied). The images are $313\times313$ lattice units. Both the transition to percolation between $\theta=0.534$ and $\theta=0.566$, and the transition to lower typical width are evident to the eye. The calculated $w_t^2$ from fig. 5 is displayed via white squares at the upper right corner of the STM images.

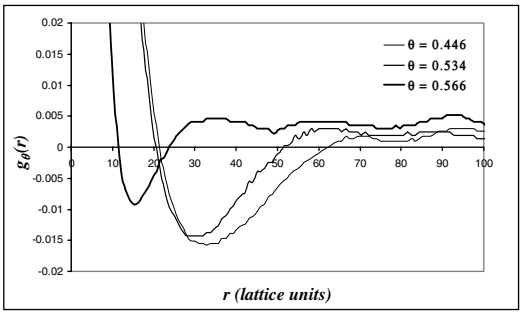


Fig. 2: The site-occupation correlation function. $g_\theta(r)$ calculated for $\theta=0.446$, $0.534<\theta_c$ and $\theta=0.556>\theta_c$. Beyond the second zero crossing, $g_\theta(r)$ is no longer correlated. The first zero gives some evaluation of the typical width $w$ for the ramified islands and it exhibit dramatic reduction above $\theta_c$.

infinite island is a fact, we merely want to verify that the overall large-scale morphology can be characterized by percolation.

In RP the structure of the percolating islands is described by the fractal concept and the fractal dimensionality $D$ of the infinite island at $\theta_c$ also represents the fractal dimension of the finite islands as long as their linear size is smaller than the correlation length $\xi$. For 2D islands

$$S\propto R_s^D,\qquad 1\ll s\leqslant s_\xi=\xi^D, \tag{2}$$

where $s$ is the islands' area and $R_s$ is the radius of gyration. The statistical distribution of the islands at percolation is described by the cluster number exponent $\tau$:

$$n_s(\theta_c)\ =s^{-\tau},\qquad p=p_c \tag{3}$$

where the cluster number $n_s$ is the probability per lattice site that a randomly chosen site belongs to a cluster of size $s$. In 2D RP $D=1.895$ and $\tau=2.05$.

The power laws (2) and (3) are asymptotic for $s\to\infty$, hence, for finite $s$, corrections to the asymptotic behavior are needed and it is custom [1] to use: $s\propto AR_s^D(1+aR_s^{-\Omega}+\text{smaller corrections})$. For the first correction term, if we plot the local slope: $\mathrm{d}\log(s)/\mathrm{d}\log(R_s)=D_{eff}$ *vs.* $\Omega aR_s^{-\Omega}/(1+aR_s^{-\Omega})$, the asymptotic value of $D$ is approached when $R_s^{-\Omega}\to0$. The exponent $\Omega$ can be derived from the data, and previous works (for example [10]) found $0.5<\Omega<1$. Figure 3 (top) is an averaged log-log plot of $s/R_s^2$ *vs.* $R_s$ with a guide line for $s\propto R_s^2$. It is apparent that the fractal behavior is restricted to islands above a crossover value, and we found it at the transition from compact to ramified islands, also indicated in fig. 5. A linear fit of the data at the fractal zone gives higher $D_{eff}$ values with increasing $\theta$ as can be seen from fig. 3 (top). Using $\Omega=0.55$ results in a linear data collapse, leading to the intersection at $D\sim1.9$ for $R_s\to\infty$ (fig. 3 (bottom)). Figure 4 is an averaged log-log plot of $n_s$ *vs.* $s$. It is evident that for large $s$ the exponent $\tau$ is being approached asymptotically. Thus, since in 2D there are only two independent exponents, we found that the large-scale behavior belongs to the universality class of RP.

In the remainder of this letter we will give a detailed analysis and discuss our main finding, that the typical island width is scaled by a factor of $e$ above $\theta_c$. We shall begin by introducing the LCM version for monolayer high 2D ramified islands.

In order to analyze the driving force leading to the width reduction above percolation, we used the LCM calculations for a simple 3D pyramid islands with width $w$, length $t$ and height $h$, experiencing shape transition above a critical area of $e^2\alpha_0^2$. We represent this transition by $w_t=e\alpha_0$ and $s_t=w_t^2$ for the transition values of the width and the area, respectively, and define

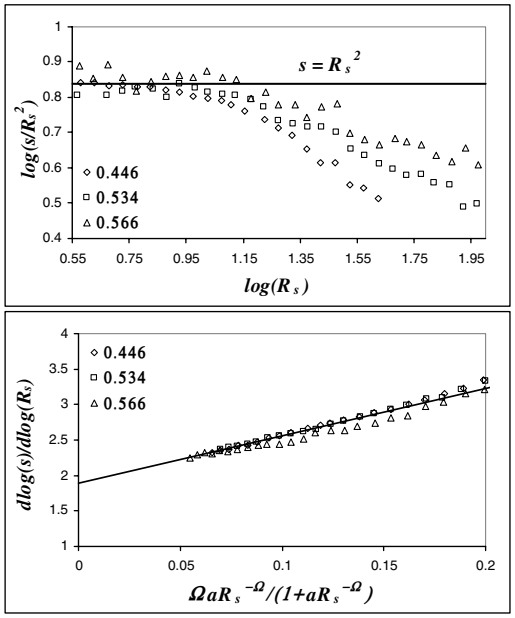


Fig. 3: The fractal dimension. Top: $\log(s/R_s^2)$ *vs.* $\log(R_s)$ shows a transition from compact ($s \propto R_s^2$) to fractal ($s \propto R_s^2$) zones ($D$ here is the effective dimension). The transition values were aligned to emphasize the increase of $D_{eff}$ with the coverage. Bottom: Evaluation of the asymptotic value by plotting of $D_{eff}$ *vs.* $\Omega a R_s^{-\Omega}/(1+aR_s^{-\Omega})$. Here, $a = 1\,\mathrm{LU}$.

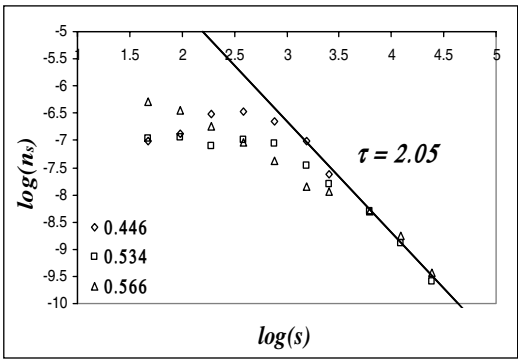


Fig. 4: The cluster number exponent $\tau$. $\log(n_s)$ *vs.* $\log(s)$ shows a convergence of $n_s$ towards $s^\tau$ for $s \to \infty$.

$w_0 \equiv \alpha_0$. The first experimental verification of this shape transition in the growth of monolayer high 2D islands was obtained by Müller *et al.* [11]. For heteroepitaxy of Cu/Ni(100), they were able to characterize the transition from compact to ramified islands by only one parameter: the arm width of the ramified islands. In this letter we shall follow their modified LCM model designed for monolayer high 2D ramified islands. For $h = 1$ they used the following expression for the total normalized energy $E$:

$$E = b(w + t) - w\ln(t) - t\ln(w), \qquad (4)$$

where the first term represents the elastic energy ($b$ is a constant consisting of elastic constants) and the other terms represent the surface energy. Since $s = wt$, (4) can be rewritten as

$$E = b(w + s/w) - w\ln(s/w) - (s/w)\ln(w). \qquad (5)$$

Minimizing the energy in (5) with respect to $w$, gives two identical solutions up to the transition value $s_t = \exp(4b+2)$, and two different solutions when $s$ exceeds this value. Above $s_t$ the width $w$ shrinks from $w_t = \exp(b+2)$ to $w_\infty = \exp(b+1)$ or $w_t/w_\infty = e$. It is customary to use a two-point correlation function [12] to characterize the microgeometry of two-phase systems. By applying it to our images, we could estimate $w$ in agreement with fig. 2, but, here we followed the footsteps of Müller *et al.*, and introduced the parameter $p$ *vs.* the island size $s$, because it predicts $w$ when the islands grow to infinity. By replacing $w$ with $p$ in (5) the dependence of $p$ on $s$ within the LCM can be obtained [11]:

$$P = 2s/w + 2w. \qquad (6)$$

Müller *et al.* were able to measure $w_t$, but they found it insensitive to the $s$ range above the transition. They proved the validity of the Tersoff and Tromp model in 2D, but, could not see the asymptotic value being approached for growing islands. This behavior had been reported later for the growth of Ag on Si(111) [13]. The value of $w$ from our data will be presented next.

Figure 5 (Top) introduces (averaged) $\log(p/s^{0.5})$ *vs.* $\log(s)$ for our three data sets: $\theta = 0.446$, $0.534 < \theta_c$ and $\theta = 0.566 > \theta_c$. The data shows a first transition from compact ($s \propto p^2$) to ramified islands. Beyond an intermediate zone the data align parallel to $s \propto p$ and this behavior can be modeled by the growth of linear chains with a typical arm width $w$. Guide lines for $s \propto p^2$ and $s \propto p$ were added to emphasize these transitions. The linear dependence of $s$ on $p$ is a familiar characteristic of the infinite island above $\theta_c$, and therefore, also of the finite but large islands that forms as $\theta$ approaches $\theta_c$. Thus, we are able to support our previous finding that on the large scales the islands can be described within the framework of RP. In our experiment for $\theta < \theta_c$ the data fall on similar curves and the transitions to compact and LC islands occur approximately at the same $w$. For $\theta > \theta_c$ the transition occurs much earlier and we receive a parallel curve at the linear chains zone, indicating the existence of a scale factor.

Figure 5 (bottom) displays $p$ *vs.* $s$ in the $s \propto p$ zone for $\theta = 0.534$ and $\theta = 0.566$. From this plot we calculated the linear chain coefficients (for $s$) $2/w$, and define these values at the LC zones by $w_t$, since, the lowest $w$ at the beginning of these zones marks exactly the transition value. We found $2/w = 0.062$ or $w_t = 32.258\,\mathrm{LU}$ for $\theta < \theta_c$, and $2/w = 0.169$ or $w_t = 11.834\,\mathrm{LU}$ for $\theta > \theta_c$. Thus, $w_t(\theta < \theta_c)/w_t(\theta > \theta_c) = 2.72$ and a factor of $e$ distinguishes the typical island widths, at the LC zone, from both sides of $\theta_c$. White squares with an area of $w_t^2$ were put in the STM images (fig. 1) to demonstrate that these typical

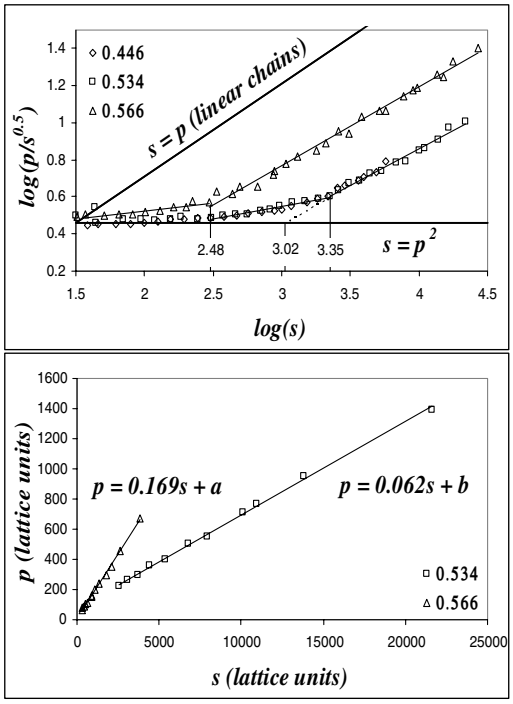


Fig. 5: The typical island width $w$. Top: $\log(p/s^{0.5})$ *vs.* $\log(s)$ shows a transition from compact ($s \propto p^2$) to LC ($s \propto p$) islands. The real 2D transitions at $\log(w) = 2.48$, 3.35 and the 1D theoretical one at $\log(w) = 3.02$ are displayed. Bottom: $p$ *vs.* $s$ for the $s \propto p$ zone. The coefficients $2/w$ for $\theta = 0.534$ and $\theta = 0.566$ are displayed.

widths are realistically estimated. We shall look more carefully into these results and discuss their connotation.

Using the value of 32.258 for $w_t$ when ($\theta < \theta_c$), we found $\log(w_t^2) = 3.02$, however, from fig. 5 (top) it is apparent that the transition to LC occurs only when $\log(w_t^2) = 3.35$ or at $w_t = 47.315\,\mathrm{LU}$. At the same time, if we mark the transition from compact to ramified islands for $\theta < \theta_c$, by $w_R$, we find $\log(w_R^2) = 2.48$ or $w_R = 17.378\,\mathrm{LU}$ and thus, $w_R = w_{LC}/e \equiv w_0$. This means that the stability of the compact island shape below $\theta_c$ begins to brake at a critical width $w_0 = 17.378\,\mathrm{LU}$, but, it is only where $w_t \equiv e w_0 = 47.315\,\mathrm{LU}$, that the islands can be described as linear chains. Instead of the sharp square-to-rectangular transition found for the 1D elongation, here, the evolution in 2D from compactness to linear chains is characterized by a transient ramified zone between $s \propto p^2$ and $s \propto p$.

The value $w_t = 32.258\,\mathrm{LU}$ calculated from the linear chain coefficient $2/w$ at $s \propto p$ can also be found if we extrapolate the linear trend line from the LC zone down to the intersection with the compact $s \propto p^2$ line at $\log(w^2) = 3.02$. We suggest that this value might refer to the theoretical value expected for 1D growth without a transition zone. The value $w_t = 47.315$ found at the transition from ramified to LC islands, refers to the real 2D value. The same 2D effect repeat itself for $\theta > \theta_c$ were the real 2D value seems to be in the vicinity of the $\theta < \theta_c$ transition value from compact to ramified islands: $\log(w^2) = 2.48$ or $w_t = 17.378\,\mathrm{LU}$ and the theoretical 1D value for $\theta > \theta_c$ at $w_t = 11.834\,\mathrm{LU}$. It is remarkable to see that, for $w_t(\theta < \theta_c)/w_t(\theta > \theta_c)$, the theoretical 1D ratio equals the real 2D ratio where $32.258/11.834 = 47.315/17.378 = 2.72 \approx e$. Together with the $w$ behavior below $\theta_c$, the general characteristics of the 1D LCM; the appearance of optimal $\alpha_0^2$ island, the shape transition above a critical $e^2\alpha_0^2$ value and the convergence back to $\alpha_0^2$ for $t \to \infty$ are reproduced for 2D ramified islands. It means that $p/s$ for 2D ramified structure constitutes of similar arms is equivalent to $p/s$ for 1D island with the same $p$ and $s$.

The most significant finding is that the transition to LC islands, or $w_t$ for $\theta > \theta_c$ occurs at the same point where the transition from compact to ramified islands, or $w_0$, occurs for $\theta < \theta_c$. Since for $\theta < \theta_c$ this transition occurs where $w_0 = w_t/e$, a factor of $e$ separates the transitions to the LC zone across $\theta_c$. Thus, analyzing the percolating island morphology by the LCM ends up with two morphological transitions. The first transition is related to the optimal tradeoff between surface energy and strain, and it appears in a gradual transition from compact to LC islands. (This optimal tradeoff freezes the structure detected, at certain coverage, even if the sample is further heated.) The second transition is related to the geometrical phase transition of percolation. Once the percolation threshold is being crossed and an infinite island is formed, $w_t$ for $\theta > \theta_c$ equals the infinite $w_\infty = w_t/e = w_0$ value for $\theta < \theta_c$, and this infinite value becomes the typical length also for finite islands.

The above nanoscale morphology characterization also suggests the existence of two typical length scales. A geometric typical length $\xi$, defined by RP, describes the morphology on the large scales as $\theta \to \theta_c$. An energetic typical length $w$, defined by the LCM, describes the effect of strain on small scale morphology. Unfortunately, experimental data with high accuracy very close to the percolation threshold are very hard to attain. Thus, the measurement to answer the interesting question of how sharp the transition of $w$ is and how it depends on $|\theta - \theta_c|$ might be a very difficult one. In the next paragraph we will backup the above result for $w_0$ with energy calculation.

To confirm the validity of the above results we made an energy calculation in order to estimate the LCM prediction for the optimal island width [3]:

$$\alpha_0 = e^{-1/2}\cot\phi\; h e^{\Gamma/ch}. \tag{7}$$

According to TT, the extra surface energy is just $2(w+t)h\Gamma$ and thus $\Gamma$ is just the step energy per surface area. We used $\Gamma = 0.14\,\mathrm{eV/atom}$ [13] and so, for an atom area of $\cong 10^{-19}\,\mathrm{m}^2$, $\Gamma \cong 0.22\,\mathrm{J/m}^2$; $h \cong 3\,\text{Å}$ is the islands height and $c = \sigma_b^2(1-\nu)/2\pi\mu$, where $\sigma_b$ is the $xx$ or $yy$ components of the bulk stress and $\nu$ and $\mu$ are the Poisson ratio and the shear modulus of the substrate. These three values are known to be $\sigma = 2.96\,\mathrm{J/m}^2$ [14] and so $\sigma_b = 0.95 \cdot 10^{-10}\,\mathrm{J/m}^3$, $\nu = 0.26$ and $\mu = 5.2 \cdot 10^{-10}\,\mathrm{N/m}^2$. $\phi$ is the contact angle and for the monolayer high islands

we used the half tetrahedral angle of 54.5° expected for monatomic steps on silicon. The above parameters give $\alpha_0 \cong 12\,\mathrm{LU}$, within 2% of our experimental value. To conclude, we shall explain how finite-size misfit makes the LCM works for homoepitaxy.

Our results confirm, for the first time, the validity of the LCM in homoepitaxy. The ability to model the formation of homoepitaxial silicon islands on Si(111)$7\times7$ with a mechanism for strain relaxation, originates from the dimension dependence of these forces. Massies and Grandjean [15] were the first ones to discover this size dependence, measuring in-plane lattice spacing oscillations (IPLSOs) by using reflection high-energy electron diffraction (RHEED). Since then, the validity of this finite size phenomenon was established, both theoretically [4–6] and experimentally [4,7,8], for heteroepitaxy as well as for homoepitaxy. Following the footsteps of Müller *et al.* [4], in heteroepitaxy, a natural misfit for semi-infinite cubic phases, an adlayer A and a substrate B, differ by their crystallographic parameters $a_0$ and $b_0$ is defined by: $m_0 = (b_0 - a_0)/a_0$. However, because of its broken bonds, a small piece of A may relax to equilibrium showing an effective lattice parameter of $a = a_0[1 + \varepsilon(h, w, t)]$ where $\varepsilon(h, w, t)$ is the size-dependent strain, referred to as the finite-size misfit or mesoscopic mismatch. Thus, a finite crystal grown on a semi-infinite substrate, has an effective misfit $m$, distinguished from the natural one as: $m \approx m_0 - \varepsilon(h, w, t)$. The finite-size misfit can be dominant also in heteroepitaxy for tiny islands and/or if $m_0$ is sufficiently small. More important for our discussion, owing to their mesoscopic mismatch, finite size 2D coherent nano homoepitexial islands for $m_0 = 0$, has to be strained by $\varepsilon(h, w, t)$ to be accommodated on their own substrate. $\varepsilon(h, w, t)$ depends only on the surface stress of the lateral and basal faces of the island, that during relaxation drags the atoms at the contact area to produce a strain field in the substrate. Müller *et al.* modeled this strain by point forces located at the edges of the islands on the substrate surface. This method is consistent with the LCM routine where TT modeled this relaxation by elastic point force monopoles acting at the islands periphery. TT also assumed a coherent Stranski-Krastanov growth with a wetting layer and so the energy of the substrate and of the islands top was considered to be equal. The homoepitaxial case is a perfect study case within the framework of this assumption.

The Si(111)$7\times7$ is familiar for possessing a reconstruction-induced stress surface [14], thus, our last remark has to do with the meaning of our results to the study of stressed surfaces. It is commonly accepted that at the steps on these surfaces one finds dipole forces, thus, strain relaxation arguments were never before applied in the study of their steps morphology. However, our results imply that for a periodic set of finite width steps, or islands, strain relaxation has to be considered. Owing to their finite size misfit and free basal surfaces we showed that strain relaxation of these islands is possible. The terraces between the islands do not have that privilege, due to their lack of the above free surfaces, and thus, elastic monopoles can emerge at the interface.

To summarize, we presented here experimental evidence for a size-dependent morphological transition with respect to the percolation threshold. Our data exhibit a reduced islands width by a factor of $e$ after the critical concentration is being crossed. This phenomenon was explained by the LCM as an asymptotic behavior when the islands grow to infinity. The asymptotic value was found at the optimal tradeoff between surface energy and strain as predicted by the LCM, hence, crossing the geometrical critical point of percolation results in a new steady-state morphology, characterized by the optimal energy width. We assert that this transition, explained for the first time using strain arguments in homoepitaxy, is a result of size-dependent mesoscopic mismatch.

* * *

We would like to thank Prof. A. Aharony for many stimulating discussions. This work was done with the support of a grant from the Israeli Academy of Science.

REFERENCES

[1] Stauffer D. and Aharony A., *Introduction to Percolation Theory* (Taylor and Francis, Philadelphia) 1992.
[2] Evans J., Thiel P. and Bartelt M., *Surf. Sci. Rep.*, **61** (2006) 1.
[3] Tersoff J. and Tromp R. M., *Phys. Rev. Lett.*, **70** (1993) 2782.
[4] Müller P., Turban P., Lapena L. and Andrieu S., *Surf. Sci.*, **488** (2001) 52.
[5] Kern R. and Müller P., *Surf. Sci.*, **392** (1997) 103.
[6] Stepanyuk V. S., Tsivlin D. V., Sander D., Hergert W. and Kirschner J., *Thin Solid Films*, **428** (2003) 1.
[7] Fassbender J., May U., Schirmer B., Jungblut R. M., Hillebrands B. and Guntherodt G., *Phys. Rev. Lett.*, **75** (1995) 4476.
[8] Turban P., Hennet L. and Andrieu S., *Surf. Sci.*, **446** (2000) 241.
[9] Wollman D. A., Dubson M. A. and Qifu Zhu, *Phys. Rev. B*, **48** (1993) 3713.
[10] Margolina A., Nakanishi H., Stauffer D. and Stanley H. E., *J. Phys. A.*, **17** (1984) 1683.
[11] Müller B., Nedelmann L. P., Fisscher B., Brune H., Barth J. V., Kern K., Erdos D. and Wollschlager J., *Surf. Rev. Lett.*, **5** (1998) 769.
[12] Blair S. C., Berge P. A. and Berryman J. G. J., *Geophys. Res.*, **101** (1996) 20359.
[13] Eaglesham D. J., White A. E., Feldman L. C., Moriya N. and Jacobson D. C., *Phys. Rev. Lett.*, **70** (1993) 1643.
[14] Martinez R. E., Augustyniak W. M. and Golovchenko J. A., *Phys. Rev. Lett.*, **64** (1990) 1035.
[15] Massies J. and Grandjean N., *Phys. Rev. Lett.*, **71** (1993) 1411.